Towards tDCS Digital Twins using Deep Learning-based Direct Estimation of Personalized Electrical Field Maps from T1-Weighted MRI

Skylar E. Stolte[1], Aprinda Indahlastari[2,3], Alejandro Albizu[2,4], Adam J. Woods[2,3,4], and Ruogu Fang[1,2,5,6⋆]

[1] J. Crayton Pruitt Family Department of Biomedical Engineering, Herbert Wertheim College of Engineering, University of Florida (UF), USA
[2] Center for Cognitive Aging and Memory, McKnight Brain Institute, UF, USA
[3] Department of Clinical and Health Psychology, College of Public Health and Health Professions, UF, USA
[4] Department of Neuroscience, College of Medicine, UF, USA
[5] Department of Electrical and Computer Engineering, Herbert Wertheim College of Engineering, UF, USA
[6] Department of Computer Information and Science and Engineering, Herbert Wertheim College of Engineering, UF, USA

Abstract. Transcranial Direct Current Stimulation (tDCS) is a non-invasive brain stimulation method that applies neuromodulatory effects to the brain via low-intensity, direct current. It has shown possible positive effects in areas such as depression, substance use disorder, anxiety, and pain. Unfortunately, mixed trial results have delayed the field's progress. Electrical current field approximation provides a way for tDCS researchers to estimate how an individual will respond to specific tDCS parameters. Publicly available physics-based stimulators have led to much progress; however, they can be error-prone, susceptible to quality issues (e.g., poor segmentation), and take multiple hours to run. Digital functional twins provide a method of estimating brain function in response to stimuli using computational methods. We seek to implement this idea for individualized tDCS. Hence, this work provides a proof-of-concept for generating electrical field maps for tDCS directly from T1-weighted magnetic resonance images (MRIs). Our deep learning method employs special loss regularizations to improve the model's generalizability and calibration across individual scans and electrode montages. Users may enter a desired electrode montage in addition to the unique MRI for a custom output. Our dataset includes 442 unique individual heads from individuals across the adult lifespan. The pipeline can generate results on the scale of minutes, unlike physics-based systems that can take 1-3 hours. Overall, our methods will help streamline the process of individual current dose estimations for improved tDCS interventions.

Keywords: transcranial direct current stimulation (tDCS) · deep learning · digital twin.

⋆ Corresponding author: ruogu.fang@ufl.edu

1 Introduction

Transcranial direct current stimulation (tDCS) is a non-invasive brain stimulation (NIBS) method that applies very weak direct current to the scalp [18]. Its primary mechanism of action is thought to be influencing cortical excitability by enacting changes on neuronal membrane potentials [18].Thus, tDCS is considered to be a neuromodulatory technique [24]. tDCS may have efficacy for interventions in ailments such as fibromyalgia, depression, anxiety, substance use disorder, stroke, Alzheimer's Disease, and pain [4,6,16,17,21]. This intervention is low-risk and cheap under conventional protocols [2]. Thus, its application paired with behavioral training is appealing compared to pharmaceuticals or invasive procedures. The United States Food and Drug Administration has not yet approved it for specific clinical indications [7]. Some other countries have approved tDCS for specific uses such as depression treatment [7].

We hypothesize that the lack of wider clinical approval is likely in part due to inconsistent findings across clinical research trials [10]. Conventional tDCS applies a fixed current and electrode placement across participants. Due to this, inconsistent findings may be partially attributed to individual factors that produce a variability in response profiles [3]. A significant source of variability derives from inter-individual anatomical differences like brain atrophy, cortical folding structures, skull thickness, and brain shape [1], [15]. These factors could cause recipients of tDCS to have widely different response rates to the same stimulation parameters. Therefore, this work begins to address this gap in tDCS research by developing a pipeline to streamline customized treatment planning.

The current methods to customize simulation primarily apply input parameters to finite element methods to produce electric field maps [15]. These field maps predict the electrical current dosages that reach the target treatment areas. Two physics-based simulators that are open access are SimNibs [20] and ROAST [11]. These tools have greatly advanced NIBS research. Yet, they do have some inherent disadvantages that could leave room for a deep learning option. For instance, simulation of one head at one set of stimulation parameters can take 1-3 hours. This can be difficult when fast turnabout is desired. Also, they may have dependencies that are not open access (e.g., ROAST on MATLAB). One previous paper demonstrated that using deep learning to generate electrical current maps for tDCS is possible [14]. This previous work, dubbed DeeptDCS, constructed an AttentionUNet network to generate electrical current maps from volume conductor models (VCMs). Their VCMs are generated using HEADRECO from SimNibs [20], whereas they superimpose a given electrode montage conductivity to give electrode context. Their dataset consists of 85 magnetic resonance images (MRIs) and 5 electrode montages. The study showed that deep learning can generate successful electrical current maps for tDCS.

Functional digital twins in neurology are computational systems that can predict brain functional changes in response to some stimuli [25]. These tools are increasingly promising with advances in artificial intelligence. We apply this idea to improve the capacity for clinical research to model tDCS parameters based on patient-wise digital twins. The current work is a significant innovation by

building a nearly real-time digital twin of the individualized brain in tDCS stimulation, without relying on additional tools. We incorporate a much larger scale dataset in terms of individual heads (n = 442). Our deep learning framework is based on SwinUNETR to take advantage of the ability of transformers to learn global spatial information [9]. Furthermore, we design special loss regularizations to improve the model's generalizability and calibration across individual scans and electrode montages. Altogether, our approach is an important contribution to creating a functional digital twin for individual response to tDCS interventions. This pipeline can help clinical research trials determine optimal individual tDCS parameters with speed, accuracy, and reliability.

2 Methodology

2.1 Dataset

Older Adult Dataset The older adult dataset is derived from a Phase III clinical trial that assessed if tDCS could improve cognition when paired with cognitive training. Specifically, our subset contains T1-weighted MRI data from 240 participants. Structural T1-MRIs were collected from two different scanner types depending on location. The main trial location used a 3-Tesla Siemens Magnetom Prisma scanner with a 64-channel head coil, whereas the secondary site used a 3-Tesla Siemens Magnetom Skyra scanner with a 32-channel head coil. Both locations used the following MPRAGE sequence parameters: repetition time = 1800 ms; echo time = 2.26 ms; flip angle = 8°; field of view = 256 × 256 × 256 mm; voxel size = 1 mm^3. All participants were cognitively healthy older adults that were between 65-89 years old at the time of the trial. Both sites' Institutional Review Boards approved the trial. Informed consent was obtained for all participants. This study obtained the permission to use the trial data.

Younger Adult Dataset The younger adult dataset is obtained from the 1200 Subject Release (S1200) from the Human Connectome Project's (HCP) Young Adult study. The latest 2017 release includes behavioral and 3T MRI data from 1,206 healthy young adult participants ages 22-35 that were collected between August 2012 - October 2015. HCP employs a protocol that is based on a customized Siemens 3T scanner called "Connectome Skyra" that is housed at Washington University in St. Louis [8]. The voxel size is given as 0.7 mm isotropic. Field of view = 260 × 311 × 260 mm. All other details are provided in their reference material [12].

2.2 Data Preparation

Reference Electrical Field Maps This work employs ROAST [11] to generate the reference electrical field maps. All standard settings for ROAST were applied other than changes in the electrode montage. We started with two common montages F3-F4 and C3-Fp2 based on previous works in tDCS research [13].

The current work started with two montages due to the time and computational resources to generate data for 470 unique MRI inputs. Follow-up work will incorporate more montages. The input current was 2 mA in amplitude. The starting dataset size encompassed three-dimensional (3D) volumetric T1-MRIs from 240 older adult participants and 230 younger adult participants. ROAST had a higher fail rate in the younger adult data, which caused the final dataset size to be about 52% older adults and 48% younger adults. The total effective data size for deep learning included 442 unique MRIs and 884 unique data pairs.

Preprocessing All images undergo preprocessing solely using Medical Open Network for Artificial Intelligence (MONAI) [5] transformations so that the final model can work on inference MRIs without other software dependencies. MONAI is an open-source framework written in Pytorch to help optimize deep learning for healthcare imaging. As such, it comes with optimized frameworks for image preprocessing, deep learning, and evaluation. Our preprocessing normalizes all MRI voxels between 0-1, crops images into $128 \times 128 \times 128$ inputs, and performs augmentation on the training data. The training data has random data flips and intensity shifts both at a probability of 0.1. The validation and testing are evaluated over the entire image inputs using $128 \times 128 \times 128$ windows using a sliding window function. The training data, validation data, and testing data encompass 708 volumes, 88 volumes, and 88 volumes, respectively. The ratio of older adults and younger adults is preserved at 52% vs. 48% in the split datasets.

2.3 Model Architecture

This work employs a dual learning scheme with regression and classification models that train simultaneously (see Fig. 1). In this approach, the regression model is the main model that generates the electrical field maps as outputs. The purpose of the classification model is to serve as an additional regularization for the regression output. It performs this task by classifying the output maps according to electrode montage type.

Regression Model The regression network performs image-to-image translation from a 3D MRI input to a 3D electrical field map output. In addition, the network is modified to input a vector that corresponds to a user's choice for the electrode montage that is used to produce the electrical field maps. SwinUNETR [9] was employed as the basic model architecture. SwinUNETR is based on the principal of combining the advantages of U-Net with those of transformer modules. The U-Net architecture has achieved state-of-the-art performance across many medical imaging tasks [19]. Even so, convolutional neural networks (CNNs) lack some ability to model global information due to the limited size of convolution kernels. Hence, the transformer modules are employed to compensate. Transformer modules have achieved increasingly high performances in natural language processing due to their attention mechanisms [23]. Like UNETR, SwinUNETR employs a transformer encoder and CNN decoder together

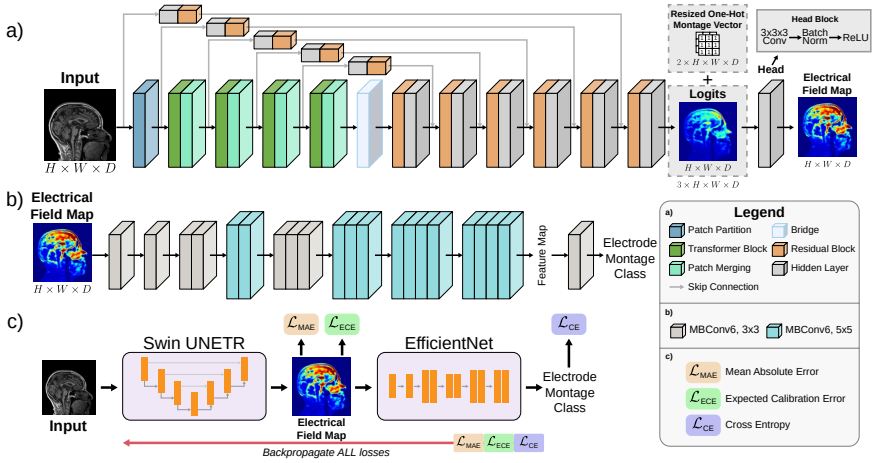

Fig. 1. Method Pipeline.

in a U-Net like structure. SwinUNETR improves UNETR by adding encoder feature extraction at five different resolutions using shifting windows.

Classification Model An additional model classifies the regression outputs into the different electrode montages. This regularizes the regression model to help further differentiate the electrical field maps that result from the same T1-weighted MRI. This work implements a custom EfficientNet [22] as the classification model. EfficientNet was originally designed to improve accuracy while conserving computational resources. It accomplishes this with a special model scaling scheme that balances network depth, width, and resolution. The design uses a mobile inverted bottleneck convolutional block that integrates squeeze-and-excitation blocks, depthwise separable convolutions, and inverted residuals.

2.4 Loss Function

The loss function (Eq. 1) contains three components to balance electrical field map accuracy, sensitivity to electrode montage type, and calibration.

$$L = \alpha \times MAE(y, \hat{y}) + \beta \times CrossEntropy(v, \hat{v}) + \gamma \times ECE(y, \hat{y}) \quad (1)$$

where y is the output electrical field map, $\hat{y}$ is the reference electrical field map, v is the output electrode montage class, and $\hat{v}$ is the true electrode montage class, and MAE is the Mean Absolute Error. ECE is the expected calibration error (Eq. 2), except we modified the standard equation for ECE to handle regression problems. Our modified equation takes the residual differences between the predicted and target values, then it bins them according to the ranges of

the predicted values. α, β, and γ are weighting terms. We use a simple grid search to establish the best weightings for each loss. The present dataset led to optimal weightings of $\alpha = 1.0$, $\beta = 0.5$, and $\gamma = 0.5$. The entire loss function is backpropagated across both the regression and classification networks.

$$ECE = \sum_{i=1}^{M} \frac{|Bin_i|}{N} \times |a_i - c_i| \tag{2}$$

Eq. 2 shows the standard equation for ECE. Confidence values are binned into M bins in which Bin_i represents the current bin. a_i is the current accuracy and c_i is the current confidence. For regression, we bin the prediction values and measure the residual error as a measure of accuracy.

2.5 Implementation

The current implementation uses 1 NVIDIA A100 GPU, 4 CPUs, and 170 Gb of RAM. The current training time on 708 data and validating on 88 data takes about 5 days of processing. The inference time for 88 testing data is less than 30 minutes, which is about 20 seconds per MRI. A batch size of 2 was used for training and validation. The model is trained with an AdamW optimizer.

3 Results

This is the first work to create a functional digital twin of tDCS directly from T1-weighted MRIs to electrical field maps, so there is no prior for comparison. Thus, this section compares the results across different parameters within our pipeline. The main evaluation metrics are Mean Absolute Error (MAE), Mean Squared Error (MSE), Structural Similarity Index Measure (SSIM), and ECE.

Ablation over Loss Terms This section demonstrates the ablation test for the three loss terms in Eq. 1. Here, $L_{MAE} = \alpha \times MAE(y, \hat{y})$, $L_{CE} = \beta \times CrossEntropy(v, \hat{v})$, and $L_{ECE} = \gamma \times ECE(y, \hat{y})$. Table 1 shows the results with different loss parameters. All other aspects of training, validation, and testing are held constant. Interestingly, table 1 shows that the highest performing algorithm is either the L_{MAE} model or the full loss model. Both of these models are fairly close for MAE and MSE, but the full model does much better for SSIM and ECE. The $L_{MAE} + LCE$ model noticeably struggles with ECE, which makes sense since L_{ECE} loss is a modified ECE term for regression. However, it is interesting that the ECE is much worse for $L_{MAE} + LCE$ compared to L_{MAE}. The $L_{MAE} + L_{ECE}$ model is better than the L_{MAE} module for ECE but worse than the full model. Fig. 2 shows the visual results for this experiment. The full model is better than the other models at capturing the correct current values in the front of the brain and at capturing detail in the back of the brain. The $L_{MAE}+LCE$ model gets the brain details correct; however, the electrical current values are predicted to be so significantly smaller than the reference that it is

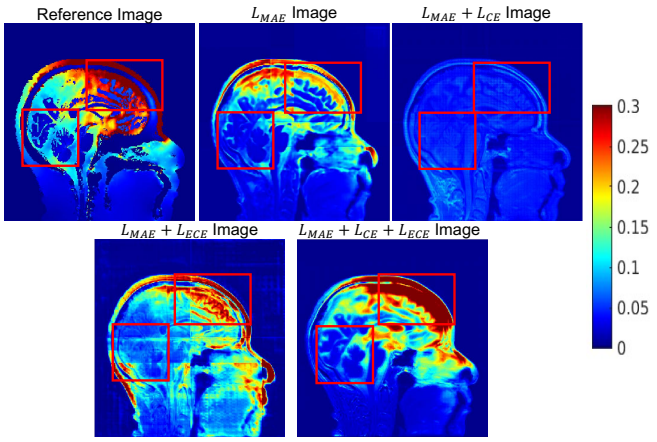

Fig. 2. Ablation test of varying loss on one older adult data and the C3-Fp2 montage.

Table 1. The performance of the ablation test for different loss configurations.

Method	MAE	MSE	SSIM	ECE
L_{MAE}	**0.03702**	**0.02727**	0.6658	0.05172
$L_{MAE} + L_{CE}$	0.04272	0.03779	0.7215	1.062
$L_{MAE} + L_{ECE}$	0.04790	0.03049	0.6078	0.04980
$L_{MAE} + L_{CE} + L_{ECE}$	0.03836	0.02754	**0.7275**	**0.04823**

hard to tell. The $L_{MAE} + L_{ECE}$ model is very noisy and includes critical errors like the electrical current in the back of the scalp area. The L_{MAE} model does indeed look the second best after the full model.

Comparison of Results across Age Cohorts Table 2 supports that the pipeline does significantly better on older adult data across all metrics. Fig. 3 displays example visual examples from both cohorts. The visual quality between cohorts does not seem to be as wide of a difference as the quantitative differences. Both samples capture the electrical current intensities the most accurately close to the front of the brain. The older adult sample does better at maintaining correct higher current intensities, especially in areas like the cerebrospinal fluid. The largest issue in this sample is that the current within the eye is overestimated. In comparison, the younger adult data correctly keeps the eye current low. However, it struggles more with underestimating the current dosage. This observation is especially true in the bottom of the brain. Interestingly, the younger adult reference seems to have a two slight noise issues in the back of the brain. The younger adult result tries to capture one of them, but it correctly misses the other. It is not clear if the different struggles between the two cohorts are due to the age range or the differences between MRI acquisition, but both of these issues are important challenges for deep learning algorithms to address before implementation.

Table 2. The performance of our method on older adults versus younger adults.

Method	MAE	MSE	SSIM	ECE
Older Adult Cohort	0.02408	0.01885	0.8208	0.02821
HCP Cohort	0.05401	0.03706	0.6254	0.07017

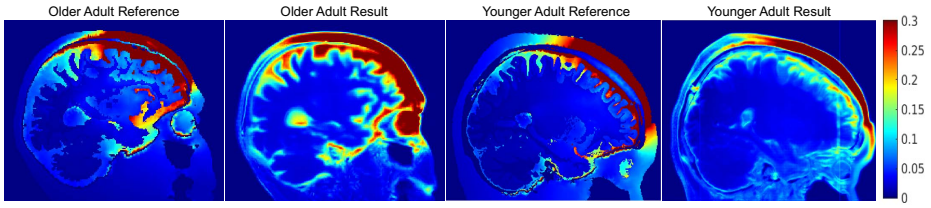

Fig. 3. Visual Samples on the HCP younger adult data and the older adult data. The F3-F4 montage is used in both.

4 Conclusions

To the best of our knowledge, this is the first work to generate electrical field simulation maps for tDCS directly from MRIs. This task is very challenging because it requires the network to capture both the brain structure and current doses. Another unique challenge is that electrical current values are very small.

Due to these challenges, the results still have room to improve before clinical implementation. Future work will examine larger changes to the regression network to fit this unique problem better. In addition, there is a discrepancy in the results from older and younger adult brains. One difference is that the older group are individuals who are at risk of age-related cognitive decline. A future experiment could use cognitive scores to match participants across age as possible. Another possibility is differences in scanner types. Training an HCP-only model with older and younger adult data could help rule out this possibility. These results could help narrow the factors that caused the performance difference.

Another limitation was that the results for direct electrical current map generation from MRIs were not yet equal to those that incorporated information like volume conductor models. Such prior results still required traditional computational modeling . The previous work was essential for tDCS research, but it cannot be used on its own. Incorporating conductivity data will address this issue without using external pipelines. We will still solely rely on MRI. The future pipeline will perform automatic segmentation, then the MRIs and the segmentations will both be used to generate electrical field maps.

A final future direction will be to validate the electrical current maps for their utility in clinical trials. The generated results will be used to predict tDCS response, and an exhaustive search will iterate through all possible tDCS parameters until positive intervention is predicted. Such experiments will incorporate more parameter combinations than the current work. The current proof-of-concept will be helpful in validating our approach for this future validation.

Overall, the current work takes important steps in achieving the goal of rapid and accurate individual modeling in tDCS using deep learning. The current study serves as an important proof-of-concept for these future works. One advantage of the current work is that it incorporates data from 442 individuals across younger and older adult data so that the modeling is robust to individual and age. This dataset is the largest for modeling electrical field maps by the number of unique individuals MRIs. Our pipeline enables users to input a desired electrode montage along with the T1. The inference time on a new T1-weighted MRI only takes 1-2 minutes, compared to physics-based simulators that can take 1-3 hours. Altogether, our method will pave the path toward individualized digital functional twins for non-invasive brain stimulation.

Acknowledgments. This work was supported by the National Institutes of Health/National Institute on Aging (NIA RF1AG071469, NIA R01AG054077), the National Science Foundation (1842473, 1908299, 2123809), the University of Florida McKnight Brain Institute, the University of Florida Center for Cognitive Aging and Memory, and the McKnight Brain Research Foundation.

Disclosure of Interests. The authors have no competing interests to declare that are relevant to the content of this article.

References

1. Albizu, A., Fang, R., Indahlastari, A., O'Shea, A., Stolte, S.E., See, K.B., Boutzoukas, E.M., Kraft, J.N., Nissim, N.R., Woods, A.J.: Machine learning and individual variability in electric field characteristics predict tdcs treatment response. Brain Stimulation **13**(6), 1753–1764 (2020). https://doi.org/10.1016/j.brs.2020.10.001
2. Bikson, M., Grossman, P., Thomas, C., Zannou, A.L., Jiang, J., Adnan, T., Mourdoukoutas, A.P., et al.: Safety of transcranial direct current stimulation: Evidence based update 2016. Brain Stimulation **9**(5), 641–661 (2016). https://doi.org/10.1016/j.brs.2016.06.004
3. Brunoni, A.R., Nitsche, M.A., Bolognini, N., Bikson, M., Wagner, T., Merabet, L., Edwards, D.J., et al.: Clinical research with transcranial direct current stimulation (tdcs): Challenges and future directions. Brain Stimulation **5**(3), 175–195 (2012). https://doi.org/10.1016/j.brs.2011.03.002
4. Butler, A.J., Shuster, M., O'Hara, E., Hurley, K., Middlebrooks, D., Guilkey, K.: A meta-analysis of the efficacy of anodal transcranial direct current stimulation for upper limb motor recovery in stroke survivors. Journal of Hand Therapy **26**(2), 162–170 (2013). https://doi.org/10.1016/j.jht.2012.07.002, epub 2012 Sep 8
5. Consortium, M.: Project monai, https://docs.monai.io/en/1.3.0/index.html, medical Open Network for AI
6. Ferrucci, R., Mameli, F., Guidi, I., Mrakic-Sposta, S., Vergari, M., Marceglia, S., Cogiamanian, F., Barbieri, S., Scarpini, E., Priori, A.: Transcranial direct current stimulation improves recognition memory in alzheimer disease. Neurology **71**(7), 493–498 (2008). https://doi.org/10.1212/01.wnl.0000317060.43722.a3

7. Fregni, F., Nitsche, M.A., Loo, C.K., Brunoni, A.R., Marangolo, P., Leite, J., Carvalho, S., Bolognini, N., Caumo, W., Paik, N.J., Simis, M., Ueda, K., Ekhtari, H., Luu, P., Tucker, D.M., Tyler, W.J., Brunelin, J., Datta, A., Juan, C.H., Venkatasubramanian, G., Boggio, P.S., Bikson, M.: Regulatory considerations for the clinical and research use of transcranial direct current stimulation (tdcs): review and recommendations from an expert panel. Clin Res Regul Aff **32**(1), 22–35 (Mar 2015). https://doi.org/10.3109/10601333.2015.980944
8. Glasser, M.F., Sotiropoulos, S.N., Wilson, J.A., Coalson, T.S., Fischl, B., Andersson, J.L., Xu, J., Jbabdi, S., Webster, M., Polimeni, J.R., Van Essen, D.C., Jenkinson, M.: The minimal preprocessing pipelines for the human connectome project. NeuroImage **80**, 105–124 (2013). https://doi.org/10.1016/j.neuroimage.2013.04.127
9. Hatamizadeh, A., Nath, V., Tang, Y., Yang, D., Roth, H., Xu, D.: Swin unetr: Swin transformers for semantic segmentation of brain tumors in mri images (2022)
10. Horvath, J., Carter, O., Forte, J.: Transcranial direct current stimulation: Five important issues we aren't discussing (but probably should be). Frontiers in Systems Neuroscience **8** (2014). https://doi.org/10.3389/fnsys.2014.00002
11. Huang, Y., Datta, A., Bikson, M., Parra, L.C.: Realistic volumetric-approach to simulate transcranial electric stimulation—roast—a fully automated open-source pipeline. Journal of Neural Engineering **16**(5), 056006 (2019). https://doi.org/10.1088/1741-2552/ab208d
12. Human Connectome Project: Wu-minn hcp 1200 subjects data release reference manual (March 1 2017), https://www.humanconnectome.org/study/hcp-young-adult/document/1200-subjects-data-release, updated April 11, 2017
13. Indahlastari, A., Albizu, A., O'Shea, A., Forbes, M.A., Nissim, N.R., Kraft, J.N., Evangelista, N.D., Hausman, H.K., Woods, A.J.: Modeling transcranial electrical stimulation in the aging brain. Brain Stimulation **13**(3), 664–674 (2020). https://doi.org/10.1016/j.brs.2020.02.007
14. Jia, X., Sayed, S.B., Hasan, N.I., Gomez, L.J., Huang, G.B., Yucel, A.C.: Deeptdcs: Deep learning-based estimation of currents induced during transcranial direct current stimulation (2022)
15. Kim, J.H., Kim, D.W., Chang, W.H., Kim, Y.H., Kim, K., Im, C.H.: Inconsistent outcomes of transcranial direct current stimulation may originate from anatomical differences among individuals: Electric field simulation using individual mri data. Neuroscience Letters **564**, 6–10 (2014). https://doi.org/10.1016/j.neulet.2014.01.054
16. Lefaucheur, J.P., et al.: Evidence-based guidelines on the therapeutic use of transcranial direct current stimulation (tdcs). Clinical Neurophysiology **128**(1), 56–92 (2017). https://doi.org/10.1016/j.clinph.2016.10.087
17. Palm, U., Hasan, A., Strube, W., et al.: tdcs for the treatment of depression: a comprehensive review. European Archives of Psychiatry and Clinical Neuroscience **266**, 681–694 (2016). https://doi.org/10.1007/s00406-016-0674-9
18. Priori, A., Berardelli, A., Rona, S., Accornero, N., Manfredi, M.: Polarization of the human motor cortex through the scalp. Neuroreport **9**(10), 2257–2260 (Jul 1998). https://doi.org/10.1097/00001756-199807130-00020
19. Ronneberger, O., Fischer, P., Brox, T.: U-net: Convolutional networks for biomedical image segmentation. In: Medical Image Computing and Computer-Assisted Intervention–MICCAI 2015: 18th International Conference, Munich, Germany, October 5-9, 2015, Proceedings, Part III 18. pp. 234–241. Springer (2015)

20. Saturnino, G.B., Puonti, O., Nielsen, J.D., Antonenko, D., Madsen, K.H., Thielscher, A.: Simnibs 2.1: a comprehensive pipeline for individualized electric field modelling for transcranial brain stimulation. Brain and human body modeling: computational human modeling at EMBC 2018 pp. 3–25 (2019)
21. Stein, D.J., Fernandes Medeiros, L., Caumo, W., Torres, I.L.: Transcranial direct current stimulation in patients with anxiety: Current perspectives. Neuropsychiatric Disease and Treatment **16**, 161–169 (2020). https://doi.org/10.2147/NDT.S195840
22. Tan, M., Le, Q.V.: Efficientnet: Rethinking model scaling for convolutional neural networks (2020)
23. Vaswani, A., Shazeer, N., Parmar, N., Uszkoreit, J., Jones, L., Gomez, A.N., Kaiser, Ł., Polosukhin, I.: Attention is all you need. Advances in neural information processing systems **30** (2017)
24. Woods, A., Antal, A., Bikson, M., Boggio, P., Brunoni, A., Celnik, P., Cohen, L., Fregni, F., Herrmann, C., Kappenman, E., Knotkova, H., Liebetanz, D., Miniussi, C., Miranda, P., Paulus, W., Priori, A., Reato, D., Stagg, C., Wenderoth, N., Nitsche, M.: A technical guide to tdcs, and related non-invasive brain stimulation tools. Clinical Neurophysiology **127**(2), 1031–1048 (2016). https://doi.org/https://doi.org/10.1016/j.clinph.2015.11.012
25. Xiong, H., Chu, C., Fan, L., Song, M., Zhang, J., Ma, Y., Zheng, R., Zhang, J., Yang, Z., Jiang, T.: The digital twin brain: A bridge between biological and artificial intelligence. Intelligent Computing **2**, 0055 (2023). https://doi.org/10.34133/icomputing.0055